

## **SDC, Materials and Methods**

### **Cell surface and intracellular phenotype staining**

Single cell suspensions were stained with fluorochrome-labeled antibodies from BioLegend recognizing the following membrane proteins: CD3 $\epsilon$  (BrilliantViolet 421 or FITC), CD4 (FITC, PerCP-Cy5.5 or APC-Cy7), CD8 (PE-Cy7 or APC-Fire750), CD25 (PE or PerCP Cy5.5), CD49d (FITC), CD127 (PE), PD1 (APC), PDL-1 (BrilliantViolet 510), OX40 (AlexaFluor 647), CCR4, CD39 (BrilliantViolet 510) and CD36 (APC/Fire750). From Thermo Fisher: LAP (eFluor 450), CD4 (APC/eFluor 480), CD86 (PE/Cy5), PDL1 (PE/Cy7), GITR (eFluor 450) and TIGIT (PE/Cy7). For intracellular IL-10, harvested cells were reactivated 4 hours with the Cell Stimulation Cocktail (ThermoFisher) without any protein transport inhibitor before fixation. For detection of intracellular targets, cells were fixed and permeabilized with the FoxP3 Fix/perm Buffer Set (BioLegend) and stained with eFluor660- or PE-labeled FoxP3 (ThermoFisher), AlexaFluor448-Helios (ThermoFisher), PE/Cyt7-CTLA-4 (BioLegend) or PE/Cy7-IL10 (ThermoFisher) antibodies. We used the fixable Zombie Violet fluorescent dye (BioLegend) to discriminate live and dead cells. LSRII cytometer (BD Biosciences) was used to acquire flow cytometry data, and data was analyzed with the FlowJo software (Tree Star).

### **Other flow cytometry analysis**

MitoTracker Green FM (Molecular Probes, Invitrogen) was used to measure mitochondrial mass following manufacturer instructions. Briefly,  $5 \times 10^5$  cells were collected, washed and stained with MitoTracker Green FM at a final concentration of



100nM in culture medium for 45 minutes at 37°C. Cells were washed with PBS, collected and analyzed by flow cytometry or further processed for additional phenotype labeling or viability staining. Results of the mitochondrial mass were expressed as mean fluorescence intensity (MFI).

$\Delta\psi_m$  was measured by TMRE staining after the incubation of the cells with 50nM TMRE (Invitrogen) in cell culture medium at 37°C for 30 minutes before immediate analysis. Each condition was tested with the corresponding control of specificity: Pretreatment of cells with the mitochondrial uncoupler FCCP (5 $\mu$ M, Sigma-Aldrich) for 10 min at 37 °C eliminates  $\Delta\psi_m$  and ensures the specificity of the  $\Delta\psi_m$  measurements.  $\Delta\psi_m$  results were expressed as the normalized TMRE loading values for mitochondrial content according to the formula:

$$\Delta\psi_m = \frac{\text{TMRE (MFI)} - \text{TMRE } preinc. \text{ with FCCP (MFI)}}{\text{MitoTracker Green FM (MFI)}}$$

Autophagy responses were monitored with the Cyto-ID Green detection reagent (Enzo Life Sciences) according to the manufacturer's instructions. The formation of autophagosomal vacuoles was assessed in 3x10<sup>5</sup> cells, collected and incubated in 200 $\mu$ L of cell culture medium for 30 min at 37°C in the dark with Cyto-ID Green at 1:1000 dilution. The enhancement of Cyto-ID Green dye signal (MFI) indicates an increase in autophagosomal vacuoles. The autophagic flux was also measured in corresponding samples by the accumulation of autophagosomes after the blockage of autophagolysosomal degradation by Chloroquine (CLQ) at 10 $\mu$ M for 6 hours before the



addition of Cyto-ID Green solution. The autophagic flux was quantified by subtracting the Cyto-ID MFI value of the sample without CLQ from the Cyto-ID MFI value of the sample with CLQ for each condition.

### **Cell lysates and western blot analysis**

Cells were harvested and lysed in 50mM TRIS-HCl (pH 7.4); 150 mM NaCl, 1% Nonidet P-40 and 0.5% n-Dodecyl- $\beta$ -D-maltoside buffer supplemented with Halt Protease inhibitor cocktail (Pierce ThermoScientific) and 1mM PMSF. Proteins from lysates corresponding to  $10^6$  cells were resolved in SDS-PAGE gels, transferred to a PVDF membrane (EMD-Millipore) and immunoblotted with the following antibodies from Cell Signaling: Anti-AKT and phospho-AKT (Serine-473); anti-4EBP1 and phospho-4EBP1 (Threonines 37/46), anti-p70S6k and phospho-p70S6k (Threonine-389), and anti-ERK1/2 and phospho-ERK2 (Threonine-202 and Tyrosine-204); anti- $\beta$ -Actin was purchased from Sigma-Aldrich. Secondary antirabbit and antimouse HRP-conjugated antibodies were obtained from Jackson ImmunoResearch Laboratories. Band densities were quantified with the ImageJ software, and the protein loading for each condition was normalized by the expression level of  $\beta$ -actin. The relative expression of proteins in RAPA- and EVR-treated cells was referred as percentage with respect to control (untreated) cells.



## Metabolic Characterization

The analyses of mitochondria oxygen consumption rates (OCR, pmol/min) and extracellular acidification rates (ECAR, mpH/min) were performed on an XF96 extracellular flux analyzer (Seahorse Bioscience, Agilent Technologies) using the protocol and conditions previously optimized for primary T cells and reported elsewhere (references #23 and #25 from the main text). Briefly, for OCR studies, T cells were harvested, washed and resuspended in XF modified DMEM media (DMEM base, 25 mM glucose, [pH 7.35]). Cells ( $4 \times 10^5$ /well), were seeded in a Cell-Tak (Corning)-coated XF-96 cell plate (Seahorse Bioscience) and incubated in a non-CO<sub>2</sub> incubator for 40 min at 37°C. A complete OCR study was performed with at least 6 replicates of each cell type and treatment and the sequential injection to each well of following solutions and final concentrations: Port A - oligomycin A (1μM); Port B – FCCP (1.5μM); Port C – Etomoxir (200μM), and Port D - mixture of Rotenone and Antimycin-A (both at 1μM). The OCR parameters were calculated from a modified version of the Report Generator XF Cell Mito Stress test (Agilent Seahorse Bioscience) to differentiate the maximal OCR fraction sensitive to etomoxir (corresponding to endogenous FA-dependent consumption) from the etomoxir-resistant (corresponding to the non-FAO rates). The rest of parameters, including baseline (basal), proton leak, ATP-linked, maximal, SRC, and nonmitochondrial respiration were calculated as AUC of specific sections of the OCR profile as detailed in the Seahorse protocol. In addition, FA-dependent fraction was calculated using the difference between the AUC OCR sums of time points in FCCP treatment (numbers 7 to 9) and in etomoxir treatment (numbers 10 to 12); FA-independent fraction was measured as the difference between the AUC OCR



sums of time points in etomoxir treatment (numbers 10 to 12) and in rotenone/antimycin treatment (numbers 13 to 15). Addition of both fractions corresponds to the maximal OCR capacity. In ECAR experiments, cells were resuspended in XF media and 3 different solutions were sequentially injected to the wells as follows: Port A – Glucose (10mM); Port B - oligomycin A (1 $\mu$ M), and Port C - 2-Deoxyglucose (2DG, at 50mM). All reagents used for injections through the ports in the Seahorse experiments were purchased from Sigma-Aldrich. The ECAR parameters were calculated with the Seahorse XF Glycolysis Stress test Report Generator (Agilent Seahorse Bioscience). Additional analyses were performed with Wave 2.2 software (Seahorse Bioscience), Excel (Microsoft Office 2013) and Prism 7.0 (GraphPad Software).

### **Suppression assay**

The suppressor activity of CD25<sup>+</sup> Treg cells was measured by the ability to inhibit the expansion of CFSE-labeled CD4<sup>+</sup> T cells. Briefly, CD4<sup>+</sup> T cells were resuspended in PBS/0.2% albumin (BSA) at a final concentration of 1 $\times$ 10<sup>6</sup> cells/mL. CFSE solution was added for a final working concentration of 2.5  $\mu$ M. After 3 min at room temperature, cell labeling was quenched by adding 3 volumes of FBS. Cells were washed 3 times in PBS/BSA and resuspended in culture medium. CFSE-labelled CD4<sup>+</sup> T cells (5 $\times$ 10<sup>4</sup> per well) were incubated with different amounts of CD25<sup>+</sup> Treg cells to generate cocultures of CFSE-labelled responder : Treg cells of 1:1, 3:1 and 10:1 ratios, in the presence of Treg Suppression Inspector beads (Miltenyi) at 2 beads per cell in a final volume of 200  $\mu$ l per well in 96-well U-bottom plates. Reference controls for suppressive activity were as follows: Negative control, with unstimulated (no beads) CFSE-labelled responders



and no Tregs; positive control, stimulated (with beads) and no Tregs, which will give the maximal proliferation of responder cells. Cocultures were harvested after 3 days of incubation and the percentage of proliferative responder cells was quantified by gating the proliferating cells (CFSE<sup>DIM</sup> responders) in flow cytometry analysis. Results are expressed in division indexes as the average number of cell divisions that a cell in the original population has undergone in the 72-h period of the assay.

### **Methylation status of the FOXP3 gene in Treg cells**

We analyzed the methylation status of 9 CpG sites in the proximal promoter region sequence corresponding to the Treg-Specific Demethylated Region (TSDR) of the intron 1 located between residues -2263 to -2330 from the transcription initiation site of FOXP3. Genomic DNA was isolated from  $4 \times 10^4$  cells for bisulfite sequencing and pyrosequencing of TSDR performed by EpigenDX (Hopkinton, MA, USA) as in previous work (ref#23 from main text).



Figure S1

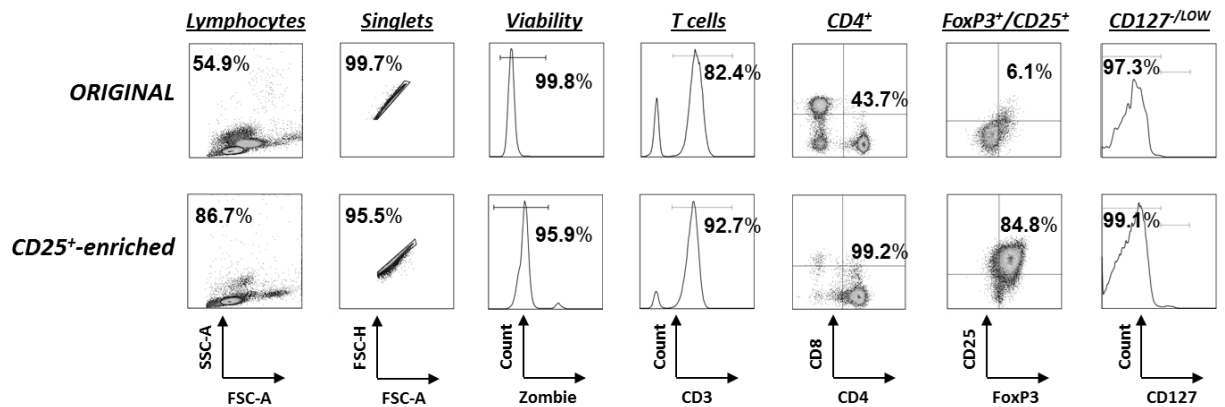


**Figure S1. Representative sequential gating strategy** used to define the population with the phenotype  $CD3^+ / CD4^+ / FoxP3^{+HIGH} / CD25^{+HIGH} / CD127^{-LOW}$  (Treg cells) from the original (TOP panels) and the CD25<sup>+</sup>-enriched fraction (BOTTOM panels) samples. Gated cells in each plot were used as the parent population in the next. The original population was obtained from PBMCs isolated from healthy adults either by leukapheresis or density gradient centrifugation. The CD25<sup>+</sup>-enriched population corresponds to the PBMCs processed through the positive selection of CD25<sup>+</sup> cells with the Clini-MACS system as detailed in the *Materials and Methods* section of the main text. The percentages of the selected (gated) populations are shown in the corresponding plot.



**Figure S2**

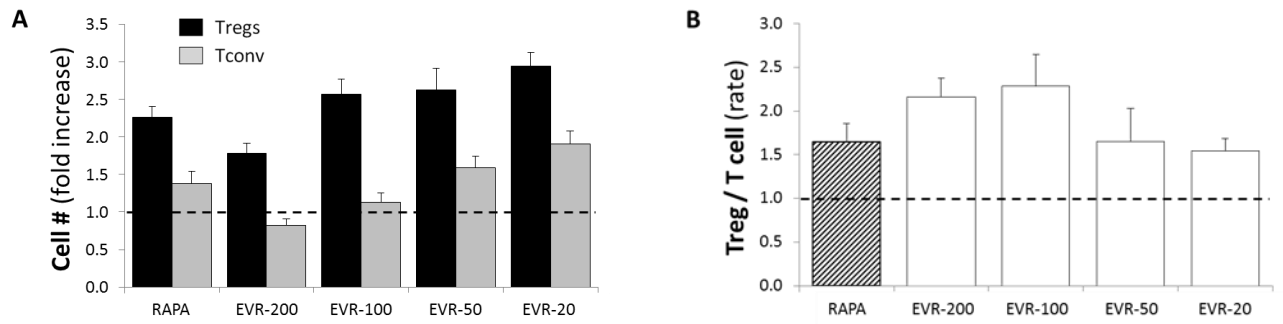


**Figure S2. Proliferative response of Treg and Tconv cells to everolimus.** The same initial number of CD25<sup>+</sup>-enriched cells (Tregs) and CD4<sup>+</sup> T cells (Tconv) were expanded for 5 days in Treg expansion medium with the addition of different doses of everolimus (EVR) or 100nM of rapamycin (RAPA). **(A)** The numbers of viable cells were measured by trypan blue exclusion and the fold-increments over the initial plated cells (dashed line) were calculated. **(B)** The same data are expressed as rates between expanded Tregs and Tconv. The results are shown as mean  $\pm$  SD (n= 3).



Figure S3

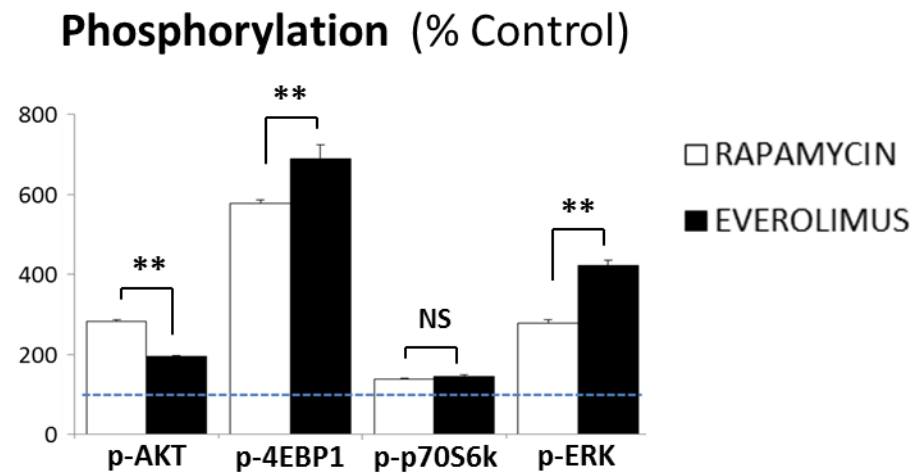


**Figure S3. Effect of rapamycin and everolimus on the regulation of protein phosphorylation of the AKT/mTOR signaling pathway in Treg cells.** The Western blot results of phosphorylated and total protein expression (Figure 1) were used to determine the effect of RAPA and EVR on the phosphorylation of AKT, 4EBP1, p70S6k, and ERK corrected for total protein expression. The results illustrate the percentage of [phosphorylated / total protein expression] index relative to untreated-control cells (leveled at 100 and depicted as a dashed line) and are shown as average  $\pm$  SD of band relative densities pooled from the same 3 different experiments ( $n=3$ ) as in Figure 1. \* $p<0.05$  and \*\* $p<0.001$  indicate significant difference between RAPA and EVR-treated cells as determined by *Wilcoxon's rank sum* test. NS indicate no significant differences between both treatments.



**Figure S4**

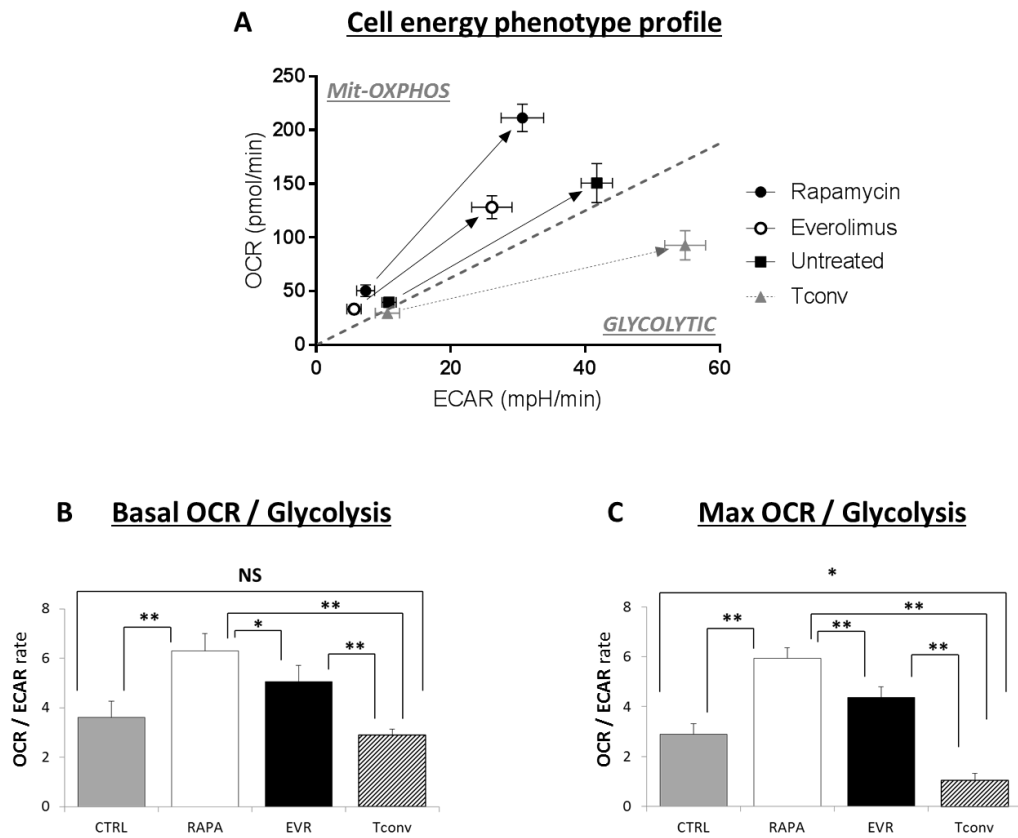


**Figure S4. Effect of rapamycin and everolimus on the bioenergetic profile of Treg cells.** (A) Oxygen consumption rates (OCR) and extracellular acidification rates (ECAR) from 5-day expanded cells were plotted against each other to illustrate the relative utilization of mitochondrial respiration and glycolysis of RARA-and EVR-treated Treg cells compared to untreated Tregs and conventional T cells (Tconv). (A) OCR plotted against ECAR show the increment of mitochondrial respiration from starting conditions (Basal) to maximal (FCCP-sensitive) OCR levels and from basal to glucose-sensitive glycolytic rates obtained from separate readouts of the same donors. Arrow lines depict the metabolic transition from basal to activated values. Data represent the



mean $\pm$ SEM pooled from 4 independent healthy donors. **(B-C)** The OCR/ECAR rates from baseline readouts and from the [FCCP sensitive mitochondrial OCR/glucose-sensitive] rates illustrated in (A) are depicted in separate bar-graph figures. It is worth noting: (1) the increased metabolic divergence between Tregs (higher OCR/ECAR rates) and Tconv (lower OCR/ECAR rates) upon the metabolic activation of the cells; (2) the increased reliance on mitochondrial respiration in RAPA- and EVR-treated compared to untreated Treg; (3) the lower energy profile of EVR-treated Treg cells compared to RAPA-treated. Statistical differences among treatments were tested by Kruskal–Wallis ANOVA followed by post hoc Wilcoxon test to assess treatment-specific differences. \* $p < 0.05$  and \*\* $p < 0.001$  indicate significant pairwise differences; NS, no significant differences.



**Figure S5**

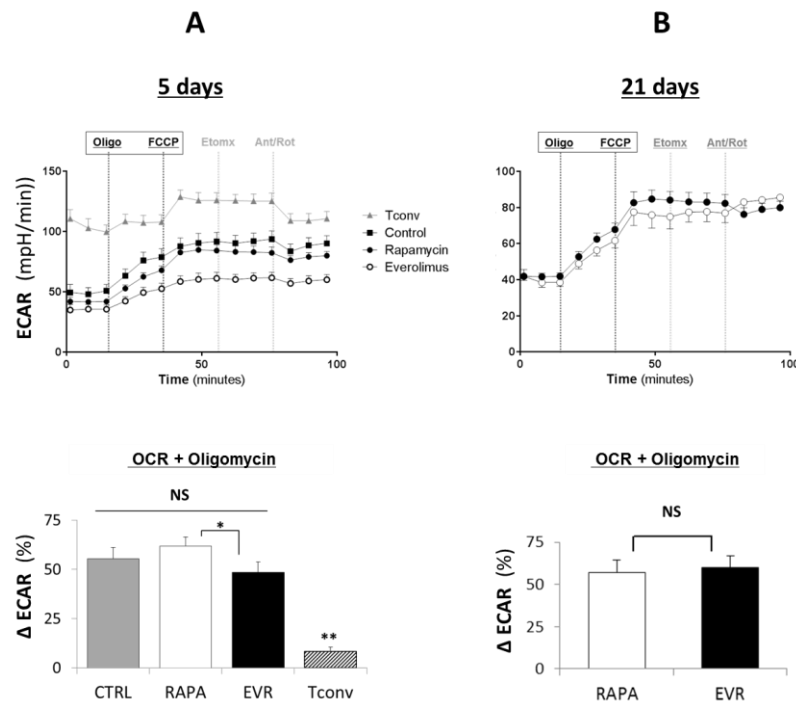


**Figure S5. ECAR data from the OCR experiments.** ECAR was measured simultaneously in the Seahorse assay with the OCR experiments corresponding to days 5 and 21 of Treg cell culture (as illustrated in Figures 2 (A) and 6 (A), respectively).

**(A)** In the 5 day-expanded Treg cells, a rapid ECAR increase cells follows the addition oligomycin, supporting the capacity of Tregs to compensate the loss of mitochondrial ATP production with the activation of the glycolytic metabolic pathway. In contrast, Tconv cells remain largely insensitive to oligomycin, which reflects a weak interplay between mitochondrial respiration and glycolysis. The bar-graph figure (BOTTOM) illustrates the increment of ECAR in response to oligomycin, and it was calculated using the difference between the area under the curve (AUC) ECAR sums of time points in oligomycin treatment (readouts 3 to 6, outlined in the time-course plot) and the AUC



ECAR sums of time points in baseline (readouts 1 to 3). Results are expressed as percentage of ECAR increment according to the formula:

$$\Delta \text{ ECAR (\%)} = 100 \times \frac{(\text{AUC Oligomycin}) - (\text{AUC Basal})}{(\text{AUC Basal})}$$

\*p<0.05 indicate a significant difference between 2 conditions as measured by *Wilcoxon's rank sum* test. The differences between rapamycin (RAPA) and everolimus (EVR)-treated cells, linked with the differences in OCR, depict the lower metabolism of EVR-treated cells in the early phase of the expansion. **(B)** The 21 day-expanded Treg cells maintain the ability to increase ECAR in response to Oligomycin. However, unlike the results from day 5, no significant differences were observed between RAPA and EVR-treated cells. These findings, together with the corresponding OCR profiles (figure 6A), depict a convergent metabolism in long-term RAPA and EVR-treated cells.



Figure S6

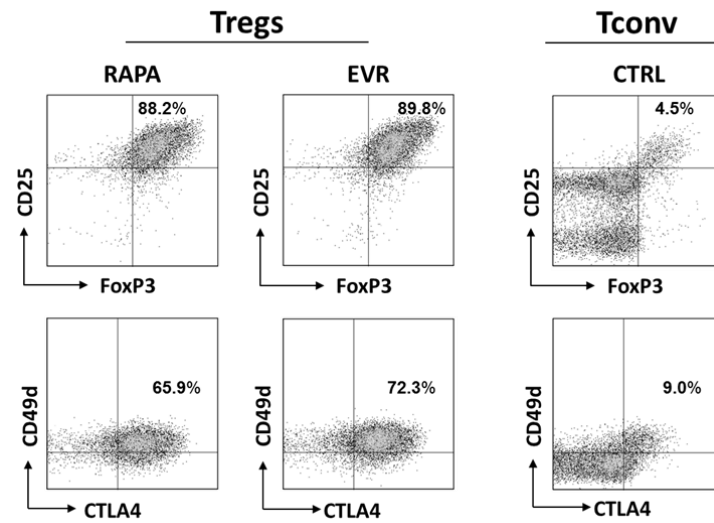


**Figure S6. Phenotypic analysis of Treg cells** treated with rapamycin (RAPA, 100nM) or everolimus (EVR, 100nM) for 5 days. Representative flow cytometry plots show that the presence of RAPA or EVR did not induce any significant phenotypic difference in Treg cells. Five day-expanded Tconv cells exhibit a different phenotypic pattern that includes a large percentage of cells expressing CD25, FoxP3 and CTLA4 markers at lower intensities compared to Treg cells.



***Figure S7***

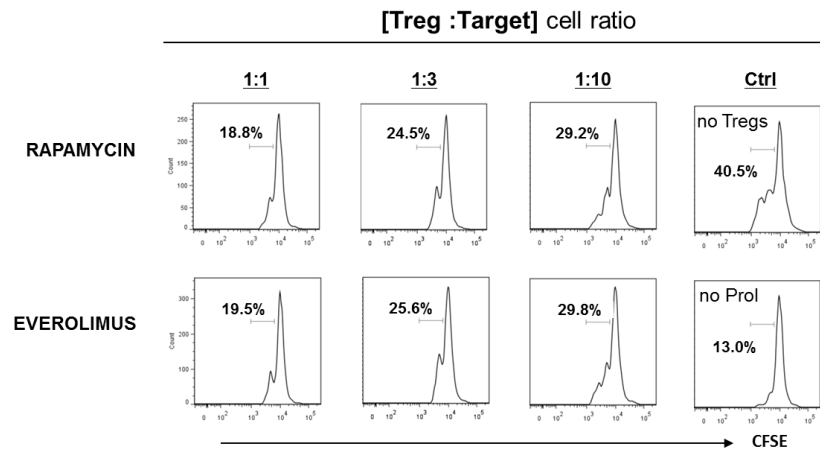


**Figure S7. Representative suppressive assay.** The suppressor activity of 5 day-expanded Treg cells was assessed in coculture with  $5 \times 10^4$  CFSE-labeled responder cells at 1:1, 1:3 and 1:10 suppressor/responder ratios in the presence of Treg Suppression Inspector beads for 72 hours. Dividing cells were identified as CFSE-dim fluorescent and showed as a numerical percentage value in each panel. Negative control was setup with unstimulated (no beads) CFSE-labelled responders alone (no Tregs), and the positive control with stimulated CFSE-labelled responder cells and no Tregs (to define the maximal proliferative response).



Figure S8

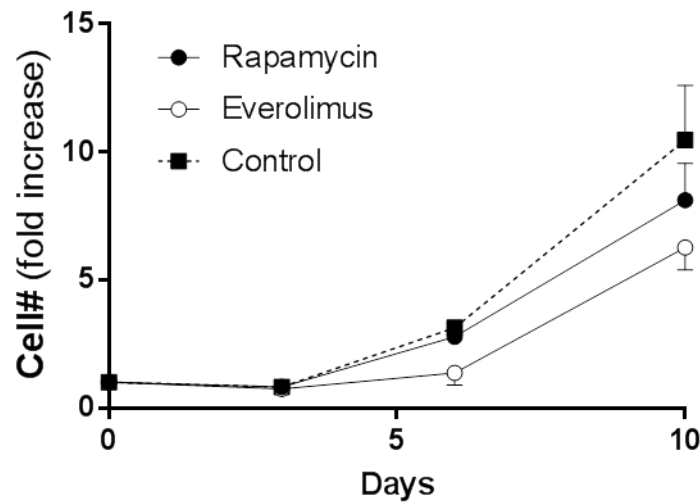


**Figure S8. Early expansion of Treg cells** –zoomed-in portion of Figure 5A- . CD4<sup>+</sup>CD25<sup>+</sup> cells were expanded in Treg expansion medium in the absence (Control, closed squares and dotted line) or in the presence of 100nM rapamycin (closed circles) or 100 nM everolimus (empty circles). The plot illustrates the temporal fold increase in cell numbers with respect to the initial seeding.



**Figure S9**

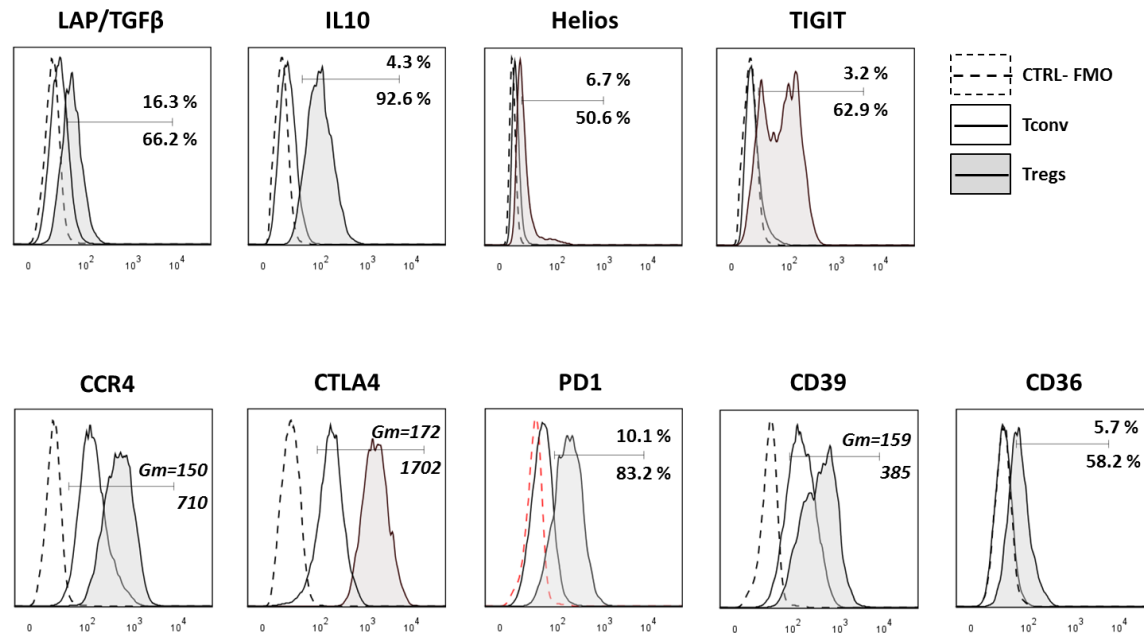


**Figure S9. Comparative phenotype analysis of expanded Tregs and Tconv cells**

The expression profiles of different proteins in Tconv (empty histogram) and Treg cells (shaded histogram) after 21-day culture in Treg expansion medium (without the addition of RAPA or EVR) were assessed by flow cytometry. The expression levels of the different proteins are indicated inside the panels as GeoMean Fluorescence Intensities (Gm) or as percentages of positive cells for Tconv (upper) and Treg (lower) cells. FMO controls are depicted as broken lines. This is a representative of 3 different experiments. The same panel of markers was subsequently evaluated in RAPA- and EVR-treated Treg cells in Figure 6B.